

“Competitive Quenching”: A Mechanism by Which Perihydroxylated Perylenequinone Photosensitizers Can Prevent Adverse Phototoxic Damage Caused by Verteporfin During Photodynamic Therapy

Gad Lavie^{*1}, Tilda Barliya¹, Mathilda Mandel¹, Michael Blank², Yonina Ron³, Arie Orenstein⁴, Tami Livnat¹, Noga Friedman⁵, Lev Weiner⁵, Mordechai Sheves⁵ and Dov Weinberger³

¹Institute of Hematology & Blood Center, Sheba Medical Center, Tel-Hashomer, Israel

²Department of Molecular Genetics and Biochemistry, Tel Aviv University, Tel Aviv, Israel

³Department of Ophthalmology, Beilinson Medical Center and Tel-Aviv University School of Medicine, Tel Aviv, Israel

⁴Center of Advanced Technology, Sheba Medical Center, Tel-Hashomer, Israel

⁵Department of Organic Chemistry, The Weizmann Institute of Science, Rehovot, Israel

Received 30 August 2006; accepted 13 March 2007; DOI: 10.1111/j.1751-1097.2007.00171.x

ABSTRACT

Incorporation of photodynamic therapy into clinical practice for induction of vascular photo-occlusion highlights the need to prevent adverse phototoxicity to sensitive juxtaposed tissues, particularly in the retina. We developed a system termed “competitive quenching” to prevent adverse phototoxic damage. It involves differential compartmentalization of a photoactivator to the intravascular compartment for photoexcitation and delivery of phototoxicity to targeted vessels. A different photodynamic agent is partitioned to the extravascular retinal space to quench reactive oxygen species generated by photosensitization, thereby protecting the adjacent retinal tissues from adverse phototoxicity. The absorption spectra of quenchers must span wavelengths that are shorter and excluded from the spectral range of photoexcitation light to prevent photoactivation of the quencher. Perihydroxylated perylenequinones were found to be suitable to function as “competitive quenchers” with the prototype hypericin identified as a potent quencher. Here we examined the mechanisms operative in competitive quenching and suggest that hypericin forms a complex with verteporfin, thereby quenching singlet oxygen formation. Furthermore, we show that hypericin, with six phenolic hydroxyls, protects retinal and endothelial hybridoma cells from phototoxicity more effectively than the dimethyl tetrahydroxy helianthone structural analog with only four such phenolic hydroxyls. The findings suggest that hydroxyl numbers contribute to the efficacy of competitive quenching.

INTRODUCTION

Photodynamic therapy (PDT) has become an accepted form of therapy in ophthalmology and is used experimentally to treat superficial tumors occurring at sites accessible to irradiation with light. Although direct toxicity to tumor cells is known to occur (1), severe damage to the microvasculature supplying the tumor is the primary cause for

effective tumor necrosis by PDT (2,3). In addition to anticancer therapy, targeting choroidal neovascularization for photoablation is the main objective in the treatment of the neovascular form of age-related macular degeneration (AMD) with PDT (4). Verteporfin (VP, VisudyneTM), a benzoporphyrin derivative, is used as the photosensitizer of choice in the treatment of AMD, being photosensitized with laser light at wavelengths > 650 nm (5,6).

The growing number of clinical indications in which PDT is being used raises the specter of adverse phototoxic damage caused to tissues adjacent to neovasculatures targeted for photoablation. This problem is more acute in AMD treated with VP-PDT. Photosensitization of the abnormal vessels takes place at close vicinity to the retinal pigment epithelium (RPE), a single layer of cells in the choroid important in preserving the function of photoreceptors. Indeed, a considerable area of weak fluorescence surrounds the choroidal neovascular complex (CNV) following PDT, which intensifies 1 week after the treatment (7). It forces ophthalmologists to minimize the light doses applied during PDT to lower the risks of irreversible phototoxic damage to the RPE. Consequently, CNVs that closed following PDT are not thoroughly eliminated and tend to recur within several weeks. Hence, protection of tissues juxtaposed to targets of PDT is a viable medical priority and can enable the use of larger and more effective light doses during therapy.

Aiming to prevent adverse phototoxicity to the RPE during PDT of CNV with VP we developed a novel approach termed “competitive quenching” (8). We found that a secondary photodynamic agent can be harnessed to function as a regulatory quencher of reactive oxygen species (ROS) generated by the photoexcited VP during PDT. We used hypericin (Fig. 1a) as the quenching photodynamic agent because of its amphi-electronic properties and ability to act as both an oxidizing as well as a reducing agent (9) mainly owing to its relatively low red/ox potential (10). The quencher must be effectively excluded from the neovascular capillaries targeted for photoablation to avoid interference with the efficacy of VP-PDT. This is achieved by compartmentalization of the quencher hypericin to the extravascular retinal and choroidal tissue. We administer hypericin first *via* the intravenous route,

*Corresponding author email: gad.lavie@sheba.health.gov.il (Gad Lavie)

© 2007 The Authors. Journal Compilation. The American Society of Photobiology 0031-8655/07

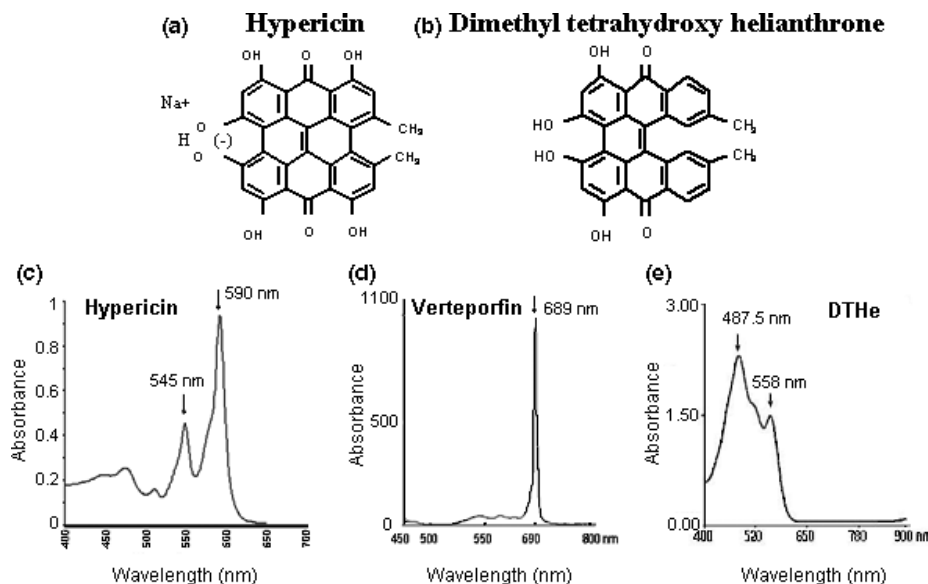


Figure 1. The chemical structures of (a) hypericin (sodium ion pair), (b) dimethyl tetrahydroxy helianthrone and the visible range absorption spectra of: (c) hypericin (in methanol), (d) verteporfin (in phosphatidylglycerol, dimyristoyl phosphatidylcholine 2:1) and (e) dimethyl tetrahydroxy helianthrone (in methanol).

allow several hours for it to extravasate, disperse in the neighboring extravascular space and clear the neovasculature targeted for ablation with PDT. Only then the effector photosensitizer VP is administered and remains confined to the intravascular compartment for the initial 30–45 min at which PDT is applied.

The quenching photodynamic agent can only function in this capacity if not photoactivated during VP-PDT. The absorption range of the quencher must, therefore, reside outside the wavelength range of light used to photoactivate the effector sensitizer and should also span wavelengths shorter than those absorbed by the photoactivated sensitizer. Hypericin is thus suitable to function as a quencher. The absorption spectrum of hypericin in the visible range, with maxima at 545 ($\epsilon \sim 22\,000\text{ M}^{-1}\text{ cm}^{-2}$) and 589 nm ($\epsilon \sim 47\,000\text{ M}^{-1}\text{ cm}^{-2}$), (Fig. 1c) (11), is safely located distantly from the absorption spectrum of VP at 689 nm (Fig. 1d) and from the laser beam cutoff value ≥ 650 nm. Hypericin is also lipophilic, a property which contributes to a relatively long tissue half-life *in vivo*.

Here we examine the mechanisms that underlie the hypericin-mediated quenching of ROS generation by VP and address some molecular requirements, which contribute to the efficacy of the competitive quenching phenomenon. Possible roles of aromatic hydroxyl groups on perylene quinones in achieving effective quenching are examined, comparing the quenching activities of hypericin with six aromatic hydroxyls (Fig. 1a) to activities of dimethyl tetrahydroxy helianthrone (DTHE), a structural analog of hypericin with four such groups (Fig. 1b). The absorption spectrum of DTHE also renders that molecule suitable to act as a quencher of ROS generated by VP (Fig. 1e). Our ultimate goal is to better understand the competitive quenching phenomenon to optimize its efficacy for clinical utilization.

MATERIALS AND METHODS

Chemicals. Hypericin (10,11-dimethyl-1,3,4,6,8,13-hexahydroxy-naphthodianthrone) and 10,13-dimethyl-1,3,4,6, tetrahydroxy-helianthrone (DTHE) were both synthesized by Dr. Y. Mazur, Department of Organic Chemistry, the Weizmann Institute of Science, Israel, as described in Lavie *et al.* (12). The compounds were dissolved in 70% aqueous ethanol to stock solutions of 2 mg mL^{-1} from which subsequent dilutions were made in sterile cell culture medium to obtain final ethanol concentrations $< 0.5\%$. VP was obtained from Novartis Ophthalmics, Hettlingen, Switzerland.

Cell lines and culture conditions. ARPE19 cells were obtained from the American Type Cell Collection (ATCC) and maintained in a medium consisting of equal volumes of HAM F-12 and Dulbecco's MEM, $40\text{ }\mu\text{M}$ glutamine, 100 U mL^{-1} penicillin and $100\text{ }\mu\text{g mL}^{-1}$ streptomycin (GibcoBRL Life Technologies Ltd, Paisley, Scotland) supplemented with 10% fetal bovine serum (FBS) (ATCC). The cells were grown in a controlled atmosphere of 37°C , 5% CO_2 . EA.hy926, a clonally pure hybridoma between human umbilical vein endothelial cells (HUVEC) and A549/8 human lung cancer cell line was obtained from Dr. C.J.S. Edgell (13), Department of Pathology, University of North Carolina, Chapel Hill. This cell line expresses many properties unique to vascular endothelial cells including production of von Willebrand factor, platelet activating factor, thrombomodulin and vitronectin receptors. The cells also produce capillary-like tubes on Matrigel (14). The EA.hy926 cell line is being used as a model for vascular endothelial cells because it provides a system of steadily proliferating cells, which are less susceptible to environmental fluctuations and senescence compared to cultured human vascular (HUVEC) or microvascular (HUMVEC) endothelial cells.

Prevention of VP-PDT-induced phototoxicity in RPE or endothelial hybridoma cells with hypericin or DTHE. Hypericin or DTHE was administered to ARPE19 or EA.hy926 cells plated 2×10^4 cells/well in 96-well flat bottom microplates (Costar, Corning, NY) for 3 h in culture (samples run in triplicates). VP was administered subsequently for two additional hours of incubation at 37°C , 5% CO_2 . Cultures that did not receive hypericin or DTHE served as positive PDT controls. The growth medium containing VP and hypericin or DTHE was removed and the cultures washed with phosphate-buffered saline (PBS). The plates were irradiated with red light using a fiber-optic noncoherent light delivery system (SeNet Ltd., Israel) in combination

with K700 broadband interference filter with central wavelengths at 700 nm and half-height bandwidth of ± 40 nm (Rolyn Optics, Covina, CA) to selectively excite VP but not hypericin or DTHE. The cultures were then returned to growth medium, cultured at 37°C, 5% CO₂ for 20 h, and cell viability was then assayed. Light fluency rate (mW cm^{-2}) was measured with a Model IL 1400A radiometer/photometer (International Light Inc., Newburyport, MA).

Cell viability analyses. Cell viability was monitored using the Hemacolor colorimetric microtiter assay that quantifies the amount of two hemacolor dyes that binds to viable adherent cells (15) and *via* the MTT assay, which measures reduction of MTT to formazan by mitochondria of viable cells (16). Formazan was quantified spectrophotometrically at 560 nm subtracting nonspecific absorption determined at 650 nm. Elevated backgrounds attributed to hypericin or DTHE at each dose level were normalized relative to cell-free blank wells containing medium and each pigment, respectively. PDT efficacy was expressed as percentage of viable cells in treated wells relative to untreated controls:

$$\% \text{ viability} = \frac{\text{OD}_{560 \text{ nm}} \text{ test sample} - \text{OD}_{650 \text{ nm}} \text{ blank}}{\text{OD}_{560 \text{ nm}} \text{ untreated control cells} - \text{OD}_{650 \text{ nm}} \text{ blank}} \times 100$$

Selective partitioning of hypericin to the extravascular retinal space and verteporfin to the intravascular compartment of the rat eye retina. Wistar rats administered with hypericin, 2 mg kg⁻¹ intravenously were anesthetized and killed after 8 h and rats administered verteporfin after 30 min. All experiments were approved by the Institutional Animal Care Committee and conducted in strict accordance with the Ministry of Health guidelines for use of animals in research. The eyes were enucleated and frozen gradually initially at -80°C and subsequently in liquid nitrogen. Frozen sections (5 μm wide) were sliced at 50 μm intervals between sections. Tissue distribution of verteporfin or hypericin was examined on unstained sections under an Olympus fluorescence microscope, to avoid washout of these photodynamic compounds from the retinal tissues during histological fixation and staining. The DuetTM multiparametric cell scanning system (BioView Corp. Nes-Ziona, Israel) equipped with an HBO103/W2, 100 W mercury lamp (Osram, Munich, Germany) and a V6200 triple color filter (Chroma, Brattleboro, VT) was used for the fluorescence analyses.

EPR, absorption and emission spectroscopies. The spin trapping studies were performed with Bruker ESR spectrometer ER 2000D-SRC at 25°C. 2,2,6,6-Tetramethyl piperidine (TEMP) was obtained from Sigma. Samples were irradiated directly inside the ESR cavity with KL 1500 lamp (Schott, Germany). Irradiation was carried out with an appropriate filter. For singlet oxygen measurements, a mixture of TEMP (0.1 M) and VP (5×10^{-5} M) was irradiated in a 70 mL ESR flat cell with or without hypericin. The highest concentration of hypericin was six equivalents relative to VP. Absorption and emission spectroscopies were measured at similar concentrations.

Statistical analyses. The Student's *t*-test was used in the statistical evaluation of the results.

RESULTS

Prevention of VP-induced phototoxicity by the diantraquinones hypericin and DTHE *in vitro*

The possibility that phenolic groups on perihydroxylated perylenequinones contribute to the quenching of ROS generated by photoactivated VP and that the quenching efficacy may correlate with the number of aromatic hydroxyl groups on the quencher has been addressed. ROS generated by photoactivated VP were quenched by hypericin, which has six aromatic hydroxyls and compared to those of DTHE, a structurally related hypericin analog with only four aromatic hydroxyls (Fig. 1b). DTHE shares some of the amphi-electronic properties that are unique to hypericin. It has a broad visible-range absorption spectrum, which spans the 450–600 nm range with peaks at 487 and 560 nm and is thus excluded from the photoexcitation range of VP (Fig. 1d).

ARPE19 cells in monolayer cultures were first loaded with 5, 10 and 20 μM of hypericin or DTHE quenchers for 3 h. VP at concentrations of 0.1, 0.25 and 0.5 $\mu\text{g mL}^{-1}$ was then administered to the cells for two additional hours of incubation, with all procedures performed in strict darkness (ambient light kept $< 0.03 \text{ mW cm}^{-2}$) to avoid photoactivation of hypericin or DTHE. All unbound VP, hypericin and DTHE were then removed by washing with PBS and the cells irradiated with 0.7 J cm⁻² of light at wavelengths of 700 \pm 40 nm in PBS, selectively photoactivating VP, which absorbs at 686 nm. This wavelength range excludes the absorption ranges of either hypericin or DTHE. The photoactivation caused VP-induced phototoxicity to the cultures. Following irradiation, the cells were washed with PBS, supplied with fresh medium and cultured at 37°C in a 5% CO₂ atmosphere for additional 20 hrs.

Protective activities from VP phototoxicity of the quenchers were measured as cell viability using the MTT assay. Figure 2a shows that in ARPE19 cells VP concentrations of 0.1, 0.25 and 0.5 $\mu\text{g mL}^{-1}$ elicit approximately 47%, 72% and 94% loss of cell viability, respectively, due to phototoxicity. However, in the presence of hypericin or DTHE, a larger percentage of cells was found to survive the VP-PDT. Percentage cell viability in the group photosensitized with 0.1 $\mu\text{g mL}^{-1}$ of VP increased

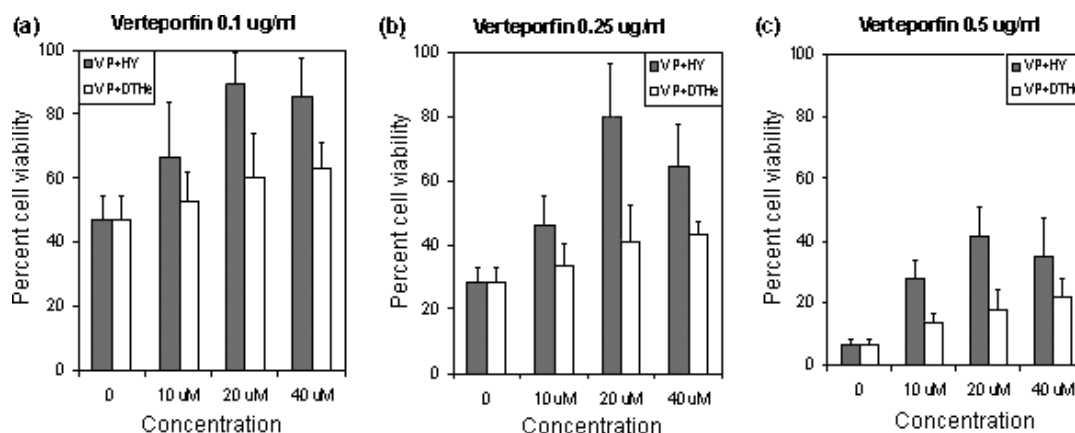


Figure 2. Protection of ARPE19 retinal pigment epithelial cells from VP-phototoxicity induced with 0.7 J cm⁻² of red light (cutoff > 650 nm), by hypericin or DTHE used as quenchers. (a) Photosensitization with 0.1 $\mu\text{g/ml}$ VP, (b) with 0.25 $\mu\text{g/ml}$ VP and (c) with 0.5 $\mu\text{g/ml}$ VP.

from 47.2% in the absence of hypericin to 66.2% ($P < 0.05$), 89.3% ($P < 0.001$) and 86.7% ($P < 0.005$) following exposure to 10, 20 and 40 μM of hypericin (referred to as HY in Fig. 2a), respectively. The corresponding increases in the percentage of viable cells in cultures that were exposed to 10, 20 and 40 μM of DTHE were only 52.3% (not statistically significant), 60.2% and 63.4% ($P < 0.05$), respectively (Fig. 2a). In these analyses hypericin was more effective in protecting the cells from VP-PDT-induced phototoxicity compared with DTHE.

Similar result patterns were obtained when PDT was performed with VP concentration of 0.25 $\mu\text{g mL}^{-1}$ (Fig. 2b). Percentage cell viability increased from 28.6% in the absence of a quencher to 46.0%, 79.5% ($P < 0.0005$) and 64.3% ($P < 0.01$) when hypericin concentrations of 10, 20 and 40 μM were applied, respectively. Here, too, the increases in viability of cells exposed to DTHE at the same molar concentrations were 33.2%, 41.3% and 43.4%, respectively, well below the protection levels achieved with hypericin. Increasing the VP concentration in the cells to 0.5 $\mu\text{g mL}^{-1}$ and photosensitizing with 0.7 J cm^{-2} of light-generated levels of phototoxicity, that were more difficult to prevent with these dianthraquinone quenchers. Nevertheless, Fig. 2c shows that even at this highly phototoxic dose, 20 μM of hypericin, was effective in preserving >40% of cell viability, although the absolute overall protection declined with the increases in the concentrations of VP. Maximal cell viability protection obtained with DTHE was >20% and achieved with 40 μM of DTHE. The findings show that although hypericin or DTHE are photodynamic molecules, they act to protect cells from phototoxicity induced by excitation of effector sensitizers such as VP at wavelengths that are longer and exclude the absorption spectral ranges of hypericin and DTHE.

Microvasculature is the primary target of PDT with VP in both AMD and in cancer therapy. The quenching of VP-PDT generated ROS and protection from phototoxicity by hypericin and DTHE have also been examined in EA.hy926 cells, a vascular endothelial hybridoma cell line that expresses a range of vascular endothelial cell properties. The results, Fig. 3a, show that exposure of EA.hy926 cells to 0.1 $\mu\text{g mL}^{-1}$ of VP and an increased dose of 1.7 J cm^{-2} of red light reduced EA.hy926 cell viability to 13.4%. The presence of hypericin at concentrations of 10 and 20 μM in the cells increased their

viability to 22% and 28%, respectively (Fig. 3a, left panel). The protection levels provided by the same molar equivalents of DTHE were 19% and 17%, respectively. Photosensitization with 0.25 $\mu\text{g mL}^{-1}$ of VP led to a decline in residual cell viability to approximately 3%; however, the presence of 10 and 20 μM of hypericin resulted in increased viability of the cells to 24% and 28.4%, respectively (Fig. 3a, middle panel). Preloading these cells with 10 and 20 μM of DTHE increased the viability of these cells only to 11.3% and 13.2%, respectively. Photosensitization with the highest VP concentration of 0.50 $\mu\text{g mL}^{-1}$ led to 100% cell death, yet the presence of hypericin preserved the viability of approximately 16–18% of the cells (Fig. 3a, right panel). DTHE protection under these conditions was negligible, confirming that hypericin protection is also superior to that provided by DTHE in the endothelial cell model.

Protection of cells from VP-mediated phototoxicity with peryhydroxylated perylenequinones was found to be more effective in ARPE19 cells compared with EA.hy926 endothelial hybridoma cells when the two were compared simultaneously in the same experiment (Fig. 3). This may result from differences in the antioxidative capacities of each cell type. To estimate the magnitude of the protection exerted by natural antioxidants we compared the effects of the natural cellular antioxidant glutathione with the quenching of ROS by hypericin in EA.hy926 endothelial hybridoma cells. Cell survival was monitored following VP-induced photosensitization. Initially, the optimal concentration of glutathione, which yields maximal inhibition of VP-PDT-mediated photocytotoxicity, was titrated and a concentration of 5 mM was found to yield the most optimal level of cell protection. We loaded EA.hy926 cells with hypericin applied at concentrations of 10 and 20 μM for 3 h in the dark or with glutathione. VP at concentrations of 0.10, 0.25 or 0.50 $\mu\text{g mL}^{-1}$ was subsequently applied to all cultures for 2 h. Cell-free reagents were removed by washing with PBS and the cells subjected to photosensitization with 0.7 J cm^{-2} of red light in PBS to generate phototoxicity. Fresh growth medium was administered, the cells were cultured for an additional 20 h and cell viability monitored by the hemacolor assay. The results, Fig. 4, show that while glutathione is the most effective in preventing phototoxicity induced with up to 0.1 $\mu\text{g mL}^{-1}$ of VP, 20 μM of hypericin was effective in maintaining similar levels of cell

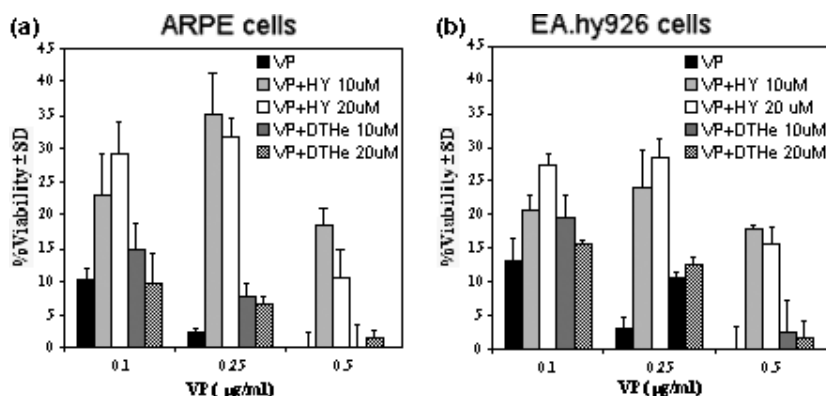


Figure 3. Comparison of the protective activities of hypericin and DTHE, from phototoxicity induced with VP and 1.7 J cm^{-2} of red light in (a) ARPE19 cells and (b) EA.hy926 endothelial hybridoma cells.

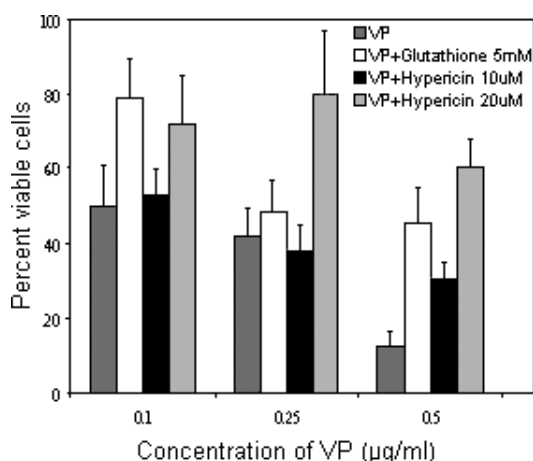


Figure 4. Comparison of efficacies of hypericin and glutathione in protecting EA.hy926 cells from phototoxicity induced by VP with 0.7 J cm^{-2} of red light.

viability, quenching ROS generated by VP concentrations of $0.25 \mu\text{g mL}^{-1}$ (Fig. 4, middle panel) and to some extent also by $0.50 \mu\text{g mL}^{-1}$ (Fig. 4, right panel).

The possibility that the effective protection of EA.hy926 cells from VP-mediated photodynamic damage by hypericin may result from interference with VP entry into these cells by

hypericin has also been examined. EA.hy926 cells were loaded with 4, 10, 20 and $40 \mu\text{M}$ of hypericin for 1 h at 37°C . VP at concentrations of 2, 5 and $10 \mu\text{g mL}^{-1}$ was then administered and allowed to enter the cells for two additional hours at 37°C . Unbound photosensitizers were removed by washing three times with PBS containing 0.5% bovine serum albumin. The cells were lysed with 0.5% buffered NP-40 and intracellular VP concentrations determined spectrofluorometrically. The results, shown in Fig. 5, indicate that VP accumulation in EA.hy926 cells remained unaltered by preloading the endothelial cells with different concentrations of hypericin, pointing away from interference with VP entry as a potential mechanism in the protection of cell viability.

Partitioning of hypericin to the extravascular retina and verteporfin to the vascular compartment

Accumulation of a dianthraquinone quencher in the extravascular choroidal and retinal space and its clearance from the vascular compartment are prerequisites for protecting the RPE and choroidal tissues from adverse phototoxicity elicited by VP leaking from neovascularization, without concomitantly interfering with the effectiveness of vessel photo-occlusion by the PDT. The feasibility of selectively partitioning hypericin to the extravascular choroidal and retinal space and VP to the vasculature of rat eyes is shown to be achievable by creating a 6–8 h lapse between the time of hypericin administration and

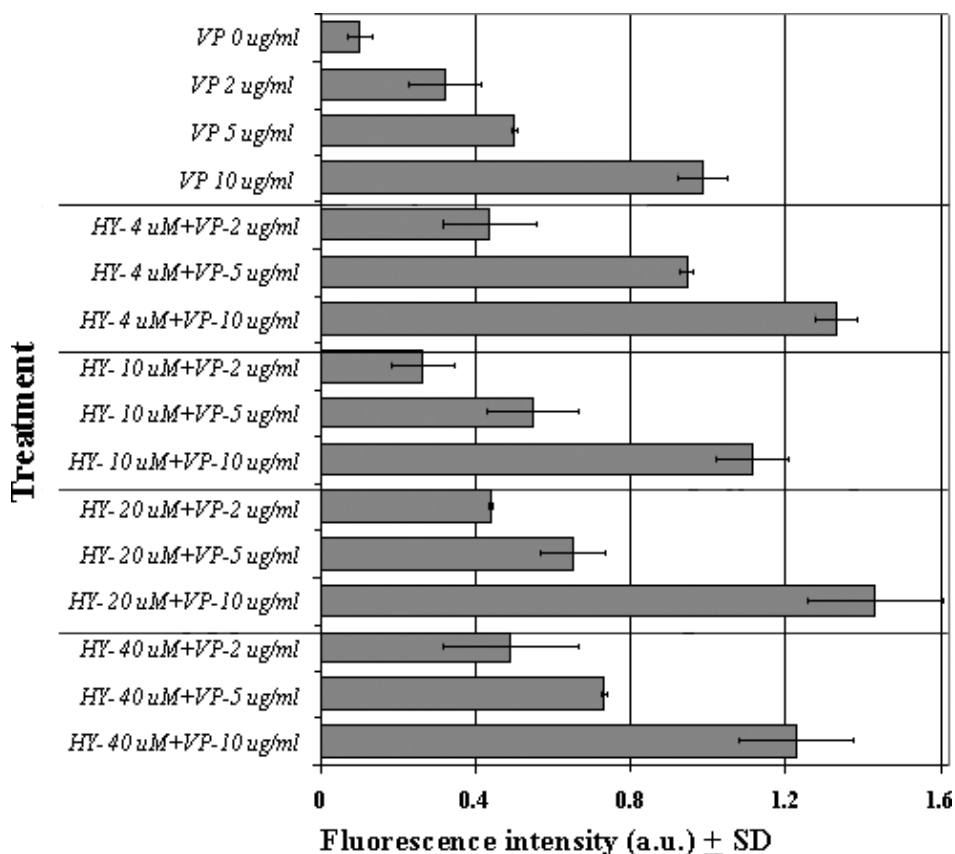


Figure 5. Hypericin does not interfere with VP entry into EA.hy926 cells. The cells were first exposed to four dose levels of hypericin. VP was subsequently administered at the indicated concentrations. Following removal of cell free dyes the cellular content of VP was determined (a.u., arbitrary units).

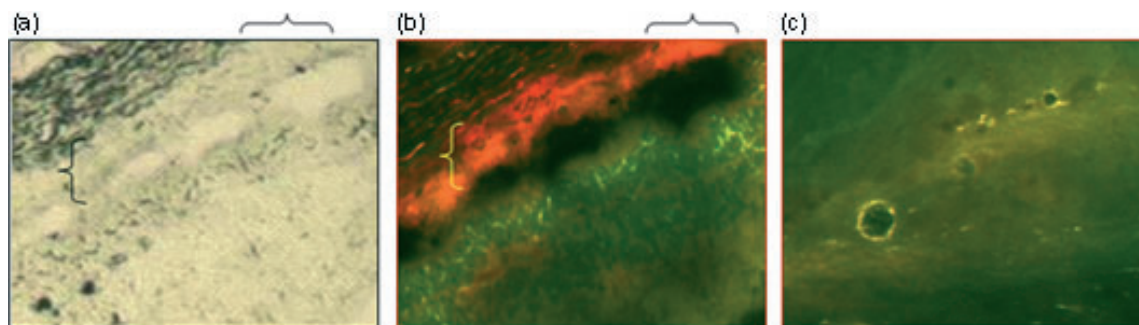


Figure 6. Microscopic analysis of sections of Wistar rat eyes prepared 8 h after administration of hypericin 2 mg kg^{-1} or 30 min after introduction of VP intravenously *via* the tail veins. Distribution of hypericin in the retina is shown. Retinae (marked area) are visualized by: (a) light field, (b) red fluorescence of hypericin marking its distribution throughout the extravascular retinal space 8 h after a single intravenous administration of hypericin 2 mg kg^{-1} . Arrows point to choroidal vessels with perivascular regions devoid of hypericin. Upper left dark area marks the sclera and the vitreous of the eye is at the lower right. (c). Section of the retina of an eye of a rat administered with VP, killed after 30 min and the eyes enucleated. VP is shown to be confined to the vascular compartment of the choroid. Light is passed through a filter with a cutoff $> 520 \text{ nm}$ (BioView imaging system; BioView Corp., Nes-Ziona, Israel) equipped with an HBO103/W2, 100 W mercury lamp (Osram, Munich, Germany) and a V6200 triple color filter (Chroma).

the subsequent injection of VP, both *via* the i.v. route. Sections prepared from the retinae and examined for hypericin fluorescence show that during these 6–8 h hypericin cleared the vasculature and was confined to the extravascular retinal space (Fig. 6b). The subsequent administration of VP allowed a time interval of $\sim 30 \text{ min}$ in which this photosensitizer remains confined to the vascular compartment (Fig. 6c). This is the time interval at which photosensitization of VP is currently being performed by ophthalmologists with a laser source emitting at $> 650 \text{ nm}$ to selectively target the choroidal neovasculature.

Evaluation of hypericin–VP interaction in solution

To assess the possible interaction between hypericin and VP and its role on singlet oxygen formation following irradiation of VP, we have used EPR spectroscopy, which is capable of monitoring production of singlet oxygen. The singlet oxygen produced is trapped by TEMP, which produces TEMPO (Scheme 1).

The central component of the triplet nitroxyl radical can be easily followed by EPR spectroscopy. Figure 7 demonstrates that following irradiation of VP (in phosphate buffer, pH 7) singlet oxygen is clearly formed. A clear effect on the singlet oxygen production was observed once the experiment was repeated in the presence of hypericin. The production of singlet

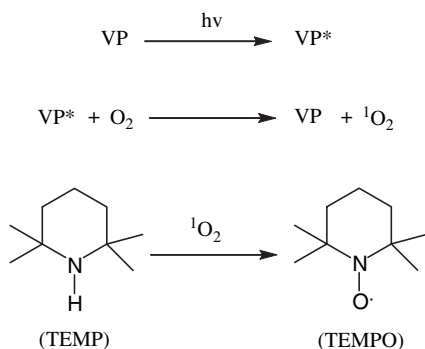
oxygen was diminished following addition of hypericin and was almost completely ceased upon increasing the hypericin concentration (Fig. 7). We note that in contrast to buffer solution, in ethanol, the addition of hypericin did not quench the singlet oxygen production and even increased it (data not shown).

To support the interaction between VP and hypericin in aqueous solution, we followed the absorption and emission spectroscopies. The absorption maximum of VP is centered at 686 nm and as shown in Fig. 8 is redshifted to 690 nm accompanied by a band broadening indicating VP–hypericin interaction. The effect was saturated at addition of about six equivalents of hypericin.

The effect of hypericin on the excited state of VP was demonstrated by the emission spectroscopy. The emission spectrum of VP is centered at 762 nm , but following addition of hypericin, this band disappeared and a much weaker band appeared at about 768 nm (Fig. 9). Thus, both absorption and emission spectroscopies indicated VP–hypericin interaction that quenches singlet oxygen production following VP irradiation as indicated by the EPR spectroscopy.

DISCUSSION

Although PDT with VP has been in clinical use for more than a decade, regulation of its phototoxic effects in sensitive adjacent tissues has thus far been unsuccessful. This shortcoming caused ophthalmologists treating choroidal neovascularization in AMD with PDT to limit the accumulation time and the dose of VP to the minimum required to achieve microvessel photo-occlusion. This is because of concern for accumulation of the VP in the adjacent choroidal and retinal tissues, where it can cause irreversible damage to these tissues. The consequences of the minimal dose and accumulation time approach are frequent disease relapses occurring several weeks after therapy, which require repeated PDT sessions. Although tissues are equipped with several stress response mechanisms and physiological antioxidants, effective PDT requires photosensitization at power density levels, which overwhelm cellular regenerative capabilities. Management of adverse phototoxic damage, which occurs during PDT, requires external support.



Scheme 1. Mechanism of TEMPO formation following VP irradiation.

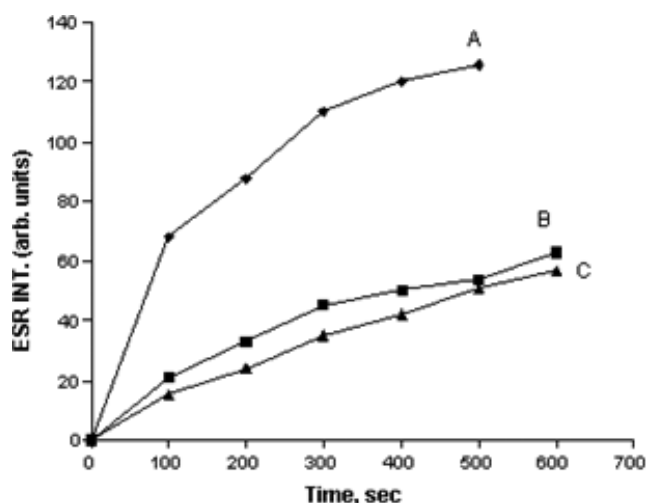


Figure 7. Effect of hypericin on singlet oxygen generation monitored by EPR spectroscopy following VP irradiation with a 650 nm cutoff filter. Singlet oxygen generation was followed by detecting the peak intensity of TEMPO ESR signal appearance: (A) VP (5×10^{-5} M) in PBS buffer; (B) addition of hypericin (20×10^{-5} M); (C) increasing hypericin concentration to (30×10^{-5} M).

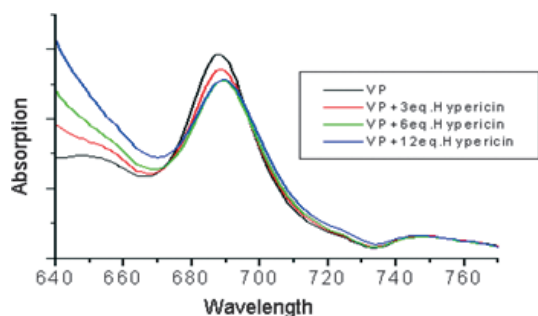


Figure 8. Effect of hypericin on the absorption spectra of VP in PBS buffer.

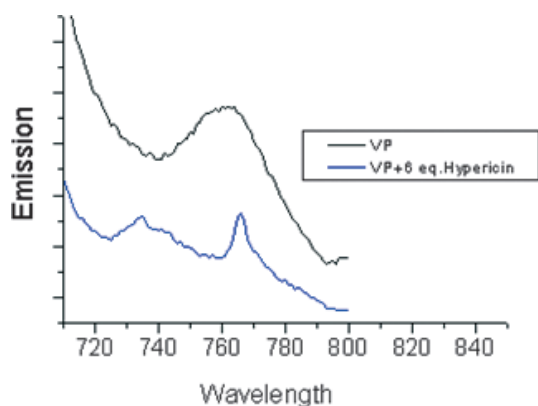


Figure 9. Emission spectra of VP in PBS buffer and its mixture with hypericin.

The dilemma of how to reconcile the contrasting needs for effective phototoxicity to a neovasculature targeted for ablation on the one hand with the need to protect adjacent tissues, particularly the single cell layer of the RPE located only microns away, remains a formidable challenge.

We addressed this problem by developing a novel approach, which combines two elements: a unique form of quenching ROS formed during laser photoexcitation of the photosensitizer. We use another photodynamic agent as quencher, the selection of which is based on red/ox potential, existence of amphi-electronic properties and absorption spectra at wavelengths, which are shorter than the absorption range of the effector photosensitizer and which are excluded from the wavelength range of the excitation light. The latter is required to prevent photoactivation of the quencher by the laser beam. Lipophilic properties in the quencher also appear to be advantageous as they contribute to a longer tissue half-life. The second element, which renders competitive quenching feasible, involves pharmacokinetic considerations to selectively partition the quencher to tissues in which collateral phototoxic damage is sought to be prevented. The selective tissue compartmentalization is important to avoid the quencher from being present in the neovascular tissue that is targeted for photoablation where it can interfere with the efficacy of the PDT (8). For example, hypericin administered intravenously to rats is confined to the intravascular compartment during the first 2 h. After 2–4 h it extravasates and is found in both the vascular and extravascular spaces of the retina whereas 6–8 h postadministration, the compound clears the circulation and is found only in the extravascular space (Fig. 6).

Verteporfin has been used as the effector photosensitizer in these studies because it is already in wide clinical use. Perihydroxylated perylenequinones are the photodynamic agents chosen as quenchers because their absorption spectra in the visible range are safely distant from that of VP at 686 nm. Hypericin (monosodium base) has maxima at 545 and 589 nm (Fig 1c) and DTHE at 487 and 558 nm (Fig 1e).

Several studies have been performed to confirm that the protection of cell viability from VP phototoxicity provided by hypericin results from quenching of ROS generated by photoactivated VP and to examine the hypothesis that VP–hypericin interaction is required to promote quenching. It has previously been suggested that VP tends to form aggregates in aqueous solutions, which might affect the photosensitization of singlet oxygen (17). It is conceivable that only the monomer fraction of VP that exists in the aqueous environment produces singlet oxygen following irradiation. The absorption and fluorescence studies performed in the present work clearly indicate that hypericin interacts with VP in aqueous solution. This interaction probably involves formation of dimers and/or larger aggregates, eliminating the monomer fraction and preventing singlet oxygen formation during photosensitization. Hypericin itself tends to form aggregates in aqueous solution. We suggest that similar interactions take place between VP and hypericin, which lead to the formation of a stable VP–hypericin complex. Another mechanism that may be considered is associated with hypericin quenching the produced singlet oxygen with no connection to formation of aggregates. However, this possibility can be ruled out as our previously described studies indicate that in ethanol solution in which a VP–hypericin complex is not formed the singlet oxygen is not quenched. Therefore, it appears that the formation of a VP–hypericin complex is required for hypericin to suppress ROS formation by photoactivated VP. The finding that intracellular hypericin does protect the viability of both ARPE19 retinal pigment epithelial and EA.hy926 cells

(Figs. 2 and 3) suggests that hypericin–VP complexes do form in biologically active environments.

The efficacy of DThe protection from VP phototoxicity is significantly weaker compared with hypericin. The weaker activity could not be attributed to differences in cellular uptake of DThe *in vitro* as DThe readily enters these and similar cell lines (11). The findings point to a direct correlation between the number of aromatic hydroxyls on a quencher photodynamic molecule and the efficacy of quenching.

Many novel and highly efficacious photodynamic agents have been developed in recent years, some of which may possibly also be useful as quenchers and prevent adverse phototoxic damage if directed to untargeted tissues. Definition of some of the properties that are required for such compounds to function as quenchers have been discussed above. It is yet to be determined whether ability to interact and form complexes with a photoactivated sensitizer is sufficient to quench its ROS-forming capability and if photodynamic properties in the quencher are of essence.

REFERENCES

- Hilf, R. (1992) Cellular targets of photodynamic therapy as a guide to mechanism. In *Photodynamic Therapy. Basic Principles and Clinical Applications* (Edited by B. W. Henderson and T. J. Dougherty), pp. 47–52. Marcel Dekker, New York.
- Star, W. M., J. P. A. Marijnissen, A. E. van den Berg-Blok, A. A. C. Versteeg, N. A. P. Franken and H. S. Rheinolds (1986) Destruction of rat mammary tumor and normal tissue microcirculation by hematoporphyrin derivative photoradiation observed *in vivo* in sandwich observation chambers. *Cancer Res.* **46**, 2532–2540.
- Fingar, V. H., T. J. Wieman, S. A. Wiehle and P. B. Cerrito (1992) The role of microvascular damage in photodynamic therapy: The effect of treatment on vessel constriction, permeability and leukocyte adhesion. *Cancer Res.* **52**, 4914–4921.
- Schmidt-Erfurth, U., S. Michels, I. Barbazetto and H. Laqua (2002) Photodynamic effects on choroidal neovascularization and physiological choroid. *Invest. Ophthalmol. Vis. Sci.* **43**, 830–841.
- Brown, S. B. and K. J. Mellish (2001) Verteporfin: A milestone in ophthalmology and photodynamic therapy. *Expert. Opin. Pharmacother.* **2**, 351–361.
- Schmidt-Erfurth, U., J. W. Miller, M. Sickenberg, H. Laqua, I. Barbazetto, E. S. Gragoudas, L. Zografos, B. Piguet, C. J. Pournaras, G. Donati, A. M. Lane, R. Birngruber, H. van den Berg, H. A. Strong, U. Manjuris, T. Gray, M. Fsadni and N. M. Bressler (1999) Photodynamic therapy with verteporfin for choroidal neovascularization caused by age-related macular degeneration: Results of retreatments in a phase 1 and 2 study. *Arch. Ophthalmol.* **117**, 1177–1187.
- Miller, J. W., U. Schmidt-Erfurth, M. Sickenberg, C. J. Pournaras, H. Laqua, I. Barbazetto, L. Zografos, B. Piguet, G. Donati, A. M. Lane, R. Birngruber, H. van den Berg, A. Strong, U. Manjuris, T. Gray, M. Fsadni, N. M. Bressler and E. S. Gragoudas (1999) Photodynamic therapy with verteporfin for choroidal neovascularization caused by age-related macular degeneration: Results of a single treatment in a phase 1 and 2 study. *Arch. Ophthalmol.* **117**, 1161–1173.
- Weinberger, D., M. Blank, Y. Ron, M. Mandel, T. Livnat, M. Lusky, T. Barliya, D. Gaaton, A. Orenstein and G. Lavie (2005) Competitive quenching: A possible novel approach in protecting RPE cells from damage during PDT. *Curr. Eye Res.* **30**, 269–277.
- Redepenning, J. and N. Tao (1993) Measurement of formal potentials for hypericin in dimethylsulfoxide. *Photochem Photobiol.* **58**, 532–535.
- Lavie, G., Y. Mazur, D. Lavie and D. Meruelo (1994) The chemical and biological properties of hypericin—A compound with a broad spectrum of biological activities. *Med. Res. Rev.* **15**, 111–119.
- Freeman, D., L. Konstantinovski and Y. Mazur (2001) The structure of hypericin in solution. Searching for hypericin's 1,6 tautomer. *Photochem. Photobiol.* **74**, 206–210.
- Lavie, G., C. Kaplinsky, A. Toren, I. Aizman, D. Meruelo, Y. Mazur and M. Mandel (1999) A photodynamic pathway to apoptosis and necrosis induced by dimethyl tetrahydroxy helianthone and hypericin in leukemic cells. Possible relevance to photodynamic therapy. *Br. J. Cancer* **79**, 423–432.
- Edgell, C. J., C. C. McDonald and J. B. Graham (1983) Permanent cell line expressing human factor VIII-related antigen established by hybridization. *Proc. Natl Acad. Sci. USA* **80**, 3734–3737.
- Rieber, A. J., H. S. Marr, M. B. Comer and C. J. Edgell (1993) Extent of differentiated gene expression in the human endothelium-derived EA.hy926 cell line. *Thromb. Haemost.* **69**, 476–480.
- Keisari, Y. (1992) A colorimetric microtiter assay for the quantitation of cytokine activity on adherent cells in tissue culture. *J. Immunol. Methods* **146**, 155–161.
- Mossman, T. (1983) Rapid colorimetric assay for cellular growth and survival: Application to proliferation and cytotoxicity assays. *J. Immunol. Methods* **65**, 55–63.
- Aveline, B. M., T. Hasan and R. W. Redmond (1995) The effects of aggregation, protein binding and cellular incorporation on the photophysical properties of benzoporphyrin derivative monoacid ring A (BPDMA). *J. Photochem. Photobiol. B, Biol.* **30**, 161–169.